Atmos. Chem. Phys. Discuss., 10, 10399–10428, 2010
www.atmos-chem-phys-discuss.net/10/10399/2010/

Atmospheric Chemistry and Physics Discussions

This discussion paper is/has been under review for the journal Atmospheric Chemistry and Physics (ACP). Please refer to the corresponding final paper in ACP if available.

Role of dust alkalinity in acid mobilization of iron

A. Ito[1] **and Y. Feng**[2]

[1]Research Institute for Global Change, JAMSTEC, Yokohama, Kanagawa, 236-0001, Japan
[2]Scripps Institution of Oceanography, University of California, San Diego, La Jolla, CA 92093-0221, USA

Received: 23 February 2010 – Accepted: 8 April 2010 – Published: 21 April 2010

Correspondence to: A. Ito (akinorii@jamstec.go.jp)

Published by Copernicus Publications on behalf of the European Geosciences Union.

Abstract

Atmospheric processing of mineral aerosols by acid gases (e.g., SO_2, HNO_3, N_2O_5, and HCl) may play a key role in the transformation of insoluble iron (Fe_2O_3) to soluble forms (e.g., Fe(II), inorganic soluble species of Fe(III), and organic complexes of iron). However, mineral dust particles also have a potential of neutralizing the acidic species due to the alkaline buffer ability of carbonate minerals (e.g., $CaCO_3$ and $MgCO_3$). Here we demonstrate the impact of dust alkalinity on the acid mobilization of iron in a three-dimensional aerosol chemistry transport model, which is incorporated with a mineral dissolution scheme. In our model simulations, most of the alkaline dust minerals cannot be entirely consumed by inorganic acids during the transport across the North Pacific Ocean. As a result, the inclusion of alkaline compounds in aqueous chemistry substantially limits the iron dissolution in aerosol solution during the long-range transport. Over the North Pacific Ocean, only a small fraction (<0.2%) of iron dissolves from hematite in the coarse-mode dust aerosols, when assuming internally mixed with carbonate minerals. However, if the iron-containing minerals are externally mixed with carbonate minerals, a significant amount (1–2%) of iron would dissolve from the acid mobilization. It implies that the alkaline content in dust aerosols might help to explain the inverse relationship between aerosol iron solubility and particle size.

1 Introduction

Iron (Fe) is an essential nutrient for marine phytoplankton (Martin et al., 1994; Mills et al., 2004). Although iron-containing soil dust mobilized from arid regions supplies majority of the iron from the atmosphere to the oceans, the key flux is the amount of soluble or bioavailable iron in terms of the biogeochemical response to atmospheric deposition (Baker and Croot, 2008; Fung et al., 2000; Jickells et al., 2005; Mahowald et al., 2009). It has been proposed that atmospheric processing of mineral aerosols by anthropogenic pollutants (mainly sulfuric acids formed from their precursors) may

ACPD
10, 10399–10428, 2010

transform insoluble iron into soluble forms (Meskhidze et al., 2003; Zhu et al., 1992; Zhuang et al., 1992).

The dissolution of dust minerals strongly depends on solution pH during the chemical processing of hematite-containing mineral dust by sulfuric acid formed from oxidation of SO_2. In a comprehensive modeling study, Meskhidze et al. (2005) developed a specific mechanism, described how the dust iron is processed by anthropogenic pollutants, and applied it to study the East Asian outflow. Solmon et al. (2009) implemented the dust iron dissolution scheme of Meskhidze et al. (2005) in a chemical transport model. Meskhidze et al. (2005) and Solmon et al. (2009) predicted insignificant amounts of soluble iron for major dust events but a significant deposition of soluble iron for smaller amounts of dust outflow during the transpacific transport. Recently, McNaughton et al. (2008) and Fairlie et al. (2009) have argued that dust does not acidify in the free troposphere except for submicron particles, because the consumption of calcite alkalinity by uptake of acid gases is slow relative to the lifetime of dust against deposition during transport across the North Pacific. Mineral aerosols originated from the Asian dust may exhibit a strong buffering ability by neutralizing acidic aerosols formed from air pollution during the long-range transport (Iwasaka et al., 1988; Song and Carmichael, 1999, 2001; Tang et al., 2004). However, only dust particles internally mixed with carbonate minerals can be buffered in this manner on an individual particle basis (Gao and Anderson, 2001). Sullivan et al. (2007) found that the submicron dust particles, which were likely associated with aluminosilicate- and iron-rich dust, could become very acidic due to mixing with sulphuric acid during the early stage of the transport.

Previous studies have suggested higher iron solubility in smaller particles (Baker and Jickells, 2006; Hand et al., 2004; Siefert et al., 1999). Baker and Jickells (2006) attributed the relationship between iron solubility and particle size to a physical control (i.e., larger surface area to volume ratio of smaller aerosol particles). However, the solubility of iron may not be such a simple function of the surface area to volume ratio (Baker and Croot, 2008; Buck et al., 2008). Smaller particles are subject to more thoroughly atmospheric processing of mineral dust due to a longer residence time, and

ACPD
10, 10399–10428, 2010

thus may result in a higher solubility (Hand et al., 2004; Zhuang et al., 1992). The dissolved iron may be chemically reactive to form smaller soluble iron particles in cloud processing (Shi et al., 2009; Zhu et al., 1992). The mineralogy of iron also influences particulate iron solubility and may contribute to the relationship due to possible variations in total iron content as a function of aerosol particle size (Claquin et al., 1999; Cwiertny et al., 2008; Journet et al., 2008; Schroth et al., 2009). Compared to mineral dust aerosols, iron from combustion sources could be more soluble, and found more frequently in smaller particles (Chuang et al., 2005; Guieu et al., 2005; Sedwick et al., 2007; Sholkovitz et al., 2009).

Here we use a global aerosol chemistry transport model to investigate the deposition of the dissolved iron during the long-range transport of mineral dust over the North Pacific Ocean. By incorporating a specific mineral aerosol dissolution scheme to the detailed aerosol chemistry model, we provide a theoretical examination of the effects of dust alkalinity on the acid mobilization of iron. In the following, Sect. 2 describes the atmospheric aerosol chemistry model, mineral aerosol dissolution scheme and iron emission data sets from both dust and combustion sources. Two numerical experiments are conducted to examine how assumptions in mixing states of mineral aerosols can affect the iron solubility. Section 3 examines the sensitivity of the soluble iron in the two simulations as well as comparisons of the model with observations. Section 4 presents a summary of our findings.

2 Model approach

2.1 Atmospheric aerosol chemistry transport model

We use the Integrated Massively Parallel Atmospheric Chemical Transport (IMPACT) model (Feng and Penner, 2007; Ito et al., 2009; Liu et al., 2005; Rotman et al., 2004) as a framework for this study. The model is driven by assimilated meteorological fields for the year of 2001 from the Goddard Earth Observation System (GEOS) of the NASA

Global Modeling and Assimilation Office (GMAO). Simulations were performed at an one-hour temporal resolution on a horizontal resolution of $2.0^{\circ} \times 2.5^{\circ}$ with 48 vertical layers for a 1-year time period with a 2-month spin-up. Emissions of primary particles and precursor gases, chemistry of gas-phase, heterogeneous, and aqueous-phase reactions, gravitational settling, dry and wet depositions, are simulated.

An online sulfur model is applied to predict the concentrations of SO_2, SO_4^{2-} (represented in 5 aerosol size bins or sections: <0.05 µm, 0.05–0.63 µm, 0.63–1.25 µm, 1.25–2.5 µm, 2.5–10 µm in radius), H_2O_2 and DMS (Liu et al., 2005). The concentrations of oxidants (i.e., HO_x ($\equiv$OH+HO_2) and O_3) are derived from a gas-phase chemistry simulation using the same emission data and meteorological fields (Ito et al., 2007, 2009). For this study, the total amount of particulate sulfate condensed on the dust in larger sizes (diameter >1.25 µm) is determined by the available surface area (Nishikawa et al., 1991; Song and Carmichael, 1999, 2001; Zhang et al., 2000). The heterogeneous uptake of nitrate and ammonium by aerosol mixtures is interactively simulated in the model using a hybrid dynamical approach (Feng and Penner, 2007). With this method, a thermodynamic equilibrium model (Jacobson, 1999) is applied to aerosols in size bin 1 (diameter <1.25 µm), while the gas and aerosol concentrations are determined by dynamically solving the mass transfer equations for particles in the 3 larger bins (diameter >1.25 µm). In the aerosol thermodynamics, sulfate, sea salt and mineral dust aerosols were assumed to be internally mixed (Feng and Penner, 2007). Thus particles in the same size bins are assumed to have the same chemical composition in aerosol mixture.

2.2 Mineral aerosol dissolution

A mineral aerosol dissolution scheme is introduced to the aerosol chemistry for the present study. We explicitly treat the dissolution/precipitation of two carbonate minerals (i.e., calcite and magnesite). The most likely clay minerals for carbonates are calcite ($CaCO_3$) and dolomite ($CaMg(CO_3)_2$) (Andronova et al., 1993; Shao et al., 2007). Ion charge balances of aerosol observed from the airborne suggest that significant

fractions of the Ca^{2+} and Mg^{2+} observed are in the form of carbonates ($CaCO_3$ and $MgCO_3$) (Maxwell-Meier et al., 2004). Since the dissolution rate of dolomite is much faster than that of magnesite ($MgCO_3$), the dissolution rate of magnesium is controlled by the dissolution of magnesite (Chou et al., 1989).

The dissolution/precipitation of the calcite ($CaCO_3$) is assumed to be in the thermodynamic equilibrium. The dissolved Ca is distributed among 4 possible different solids ($CaCO_3$, $CaSO_4$, $Ca(NO_3)_2$, and $CaCl_2$) or the aqueous-phase species (Ca^{2+}). The relative amounts of each of these species are calculated interactively by the thermodynamic module (Jacobson, 1999).

Magnesite ($MgCO_3$) dissolution is treated explicitly as a kinetic process depending on pH, chemical composition and temperature of the dust coating solution. For kinetically-controlled dissolution rate of mineral (R_i), we adopt the formulation of Lasaga et al. (1994):

$$R_i = K_i(T) \times a(H^+)^{m_i} \times \quad f(\Delta G_i) \times A_i \times W_i \tag{1}$$

where K_i is the temperature (T) dependent reaction coefficient (moles dissolved m^{-2} of mineral s^{-1}) for mineral i, $a(H^+)$ is the H^+ activity, m_i is an empirical parameter, f is a function of Gibbs free energy change of a particular mineral dissolution reaction (ΔG_i), which accounts for the variation of the rate with deviation from the equilibrium (Cama et al., 1999), A_i is the specific surface area of mineral aerosols in units of $m^2\,g^{-1}$, and W_i is the weight fraction of the mineral in dust in units of g of mineral (g of dust)$^{-1}$. Values for K_i, m_i, A_i, and W_i for each of the mineral-dissolution reactions considered here are listed in Table 1. The function f is in turn given by

$$f(\Delta G_i) = 1 - \exp[(n \times \Delta G_i)/(R \times T)] \tag{2}$$

where

$$\Delta G_i = R \times T \times \ln(Q_i/KEQ_i) \tag{3}$$

and n is an empirical parameter that in mineral-fluid reaction kinetics is most commonly set to 1 (e.g., Burch et al., 1993), R is the gas constant, Q_i is the reaction activity

quotient (i.e., the ratio of the product of the reactants over the product of the species produced), and KEQ_i is the equilibrium constant (Meng et al., 1995). Values of the kinetic constants for the magnesite dissolution are available from Chou et al. (1989) (Table 1). In highly acidic solutions, rates are independent of pH in the case of relatively fast dissolving minerals such as carbonates (Pokrovsky and Schott, 1999). Thus we set pH=3 for the calculation of dissolution rates when pH<3. The precipitation of secondary compounds ($MeSO_4$, $Me(NO_3)_2$, and $MeCl_2$, Me=Ca and Mg) is assumed to be an irreversible reaction (Dentener et al., 1996; McNaughton et al., 2008; Song and Carmichael, 1999, 2001).

The hematite dissolution is also treated explicitly as a kinetic process, after Meskhidze et al. (2005). The three-stage kinetic process is considered for specification of hematite dissolution constant, depending on the total amount of the hematite dissolved. The first (0–0.8% of total oxide dissolved) and third (40–100% of total oxide dissolved) stages are relatively slow dissolution compared to the second stage (0.8–40% of total oxide dissolved). Since the dissolution rate of hematite is very slow, the system always remains far from equilibrium under our experimental conditions, hence no backward reaction is considered (i.e., $f(\Delta G_i)=1$).

2.3 Iron emission

We compiled an emission inventory of iron from dust and combustion sources (Fig. 1). The Gobi (northern China and southern Mongolia) and Taklimakan (western China) deserts are the dominant source regions of dust in East Asia during springtime (Sun et al., 2001). On the other hand, combustion sources show a broad distribution across rural areas of China, where domestic coal combustion is prevalent (Streets et al., 2003).

For the simulation of mineral aerosols, we use the dust emissions compiled by Dentener et al. (2006). The dust emission fluxes were interpolated and represented in the 4 size bins (0.05–0.63 µm, 0.63–1.25 µm, 1.25–2.5 µm, 2.5–10 µm in radius) (Liu et al., 2005). Currently, the iron-containing mineral in dust aerosol is treated as hematite, following previous studies (Luo et al., 2008; Meskhidze et al., 2005; Solmon et al., 2009).

Thus the chemical composition of dust aerosols is assumed to be: 11% $CaCO_3$, 5.5% $MgCO_3$, and 5% Fe_2O_3 (59 Tg Fe per year) (Duce and Tindale, 1991; Gillette et al., 1993; Meskhidze et al., 2005; McNaughton et al., 2008).

Iron from combustion sources could have a pronounced effect on aerosol iron solubility in addition to mineral dust aerosols (Chuang et al., 2005; Luo et al., 2008; Schroth et al., 2009). For emissions of iron from combustion sources for 2001 (1.2 Tg Fe per year), we use fuel consumption data and specific emission factors for different fuel use categories to develop an inventory, based on particulate emissions estimates from Ito and Penner (2005) and emission factors complied by Luo et al. (2008). We use conservative values of iron fractions in minerals (Table 2). We assume that the inorganic matter consists of materials that are not black carbon and organic matter. Thus the iron contents in the fine and coarse particles do not exceed the amounts of inorganic matter. We use 4% and 0.45% soluble iron fractions for the combustion and dust sources at the initial conditions, respectively, following Luo et al. (2008). The fine iron particle from combustion sources is transported similar to black carbon in the model, while the large-particle distribution is treated here as a single particle mode (dust size bin 4).

3 Model sensitivity analysis

Two separate simulations were performed with and without the alkaline dust in the aqueous chemistry. In the first simulations (Exp1), carbonate dust minerals ($MeCO_3$, Me=Ca and Mg) react with inorganic acids (H_2SO_4, HNO_3, and HCl) from the air pollution, which form thermodynamically more stable materials ($MeSO_4$, $Me(NO_3)_2$, and $MeCl_2$). Thus, the dust alkalinity reservoir is able to buffer the acidity linked to anthropogenic emissions, although the pH buffering capacity of the original dust particles might be compromised especially for submicron particles in the long-range transport. On the other hand, if dust without carbonate minerals (in the second sensitivity simulations, Exp2) mixes with sulphate, it can be acidified (Sullivan et al., 2007). Iron content in this type of dust in the atmosphere may be structurally associated with

aluminosilicate minerals, and potentially represent a significant source of soluble iron in acidic environments (Cwiertny et al., 2008; Journet et al., 2008; Schroth et al., 2009).

3.1 Dust alkalinity

Since calcite dissolves much faster than magnesite, it is the main contributor to the buffering effect of dust that neutralizes acidic aerosols formed from air pollution in the long-range transport. In the model simulations including the alkaline dust in the aqueous chemistry (Exp1), the soluble calcium (i.e. sum of calcite and calcium ion) is being converted to solid forms, as dust particles travel from the source regions in East Asia to the eastern North Pacific Ocean, as shown for April in Fig. 2. The estimated fraction (%) of the soluble calcium in total calcium is significantly different between the surface air (Fig. 2a) and free troposphere (Fig. 2b). The low-altitude dust aged faster than the high-altitude dust, as a result of the high pollutant loadings near the surface (Tang et al., 2004). However, the simulated alkaline dust are only partly consumed by acids both at the surface (60–80%) and in the free troposphere (20–40%) during the transport, which are consistent with the observations at the ground sites (Arimoto et al., 2004) and in the free troposphere (McNaughton et al., 2008), respectively. In the surface air, the percentage of the modeled soluble calcium is reduced from 90–100% near the source region to 60–70% at a regional sampling site (GOSAN) located on the west-end of Jeju Island, south of the Korean Peninsula. In the free troposphere, large fractions of the mineral dust (80–90%) remain as soluble calcium over Japan, and then only 20–40% of the soluble calcium is converted to solids ($CaSO_4$, $Ca(NO_3)_2$, and $CaCl_2$) over the eastern North Pacific.

3.2 Iron solubility

The model simulations demonstrate a substantial reduction in the dissolved iron fraction (DIF) in dust when aerosol carbonate chemistry is included (Fig. 3). Here, the DIF in dust (%) was calculated using the total iron concentration from dust sources only.

The emissions of alkaline gas (i.e., ammonia) exceed the amount that is needed to neutralize sulfate and nitrate in large portions of East Asia (Tang et al., 2004). In our model calculations, a relatively high pH (>3), which may hinder the hematite (Fe_2O_3) dissolution, is predicted over the ammonia source regions (Fig. 4). In the absence of alkaline dust (Exp2), lower pH (<3) is predicted near both the dust and sulfuric gas source regions. When aerosol carbonate chemistry is included (Exp1), however, the calcite-rich dust does not acidify near the dust source regions due to the buffering ability of carbonate minerals. Thus the iron-containing mineral aerosols in Exp2 dissolve faster than those in Exp1, and also dissolve faster in some regions due to an accelerated dissolution rate at the second stage (Fig. 5).

Measurements sampled at the GOSAN station (33°17′ N, 126°10′ E) from 31 March to 2 May in 2001 have shown four distinct high water-soluble fraction of iron in the total suspended particles (6.45–12%) during the time periods when the air masses originate from Japan (Duvall et al., 2008). Model results of the iron fractional solubility (Exp1 and 2) underestimate the mean and standard deviation when these values are included for the comparison (Table 3). Here, the fractional solubility of aerosol iron (%) was calculated using the total iron concentration from both dust and combustion sources. However, the comparison excluding them shows good agreement in the averaged iron fractional solubility (1.4% for Exp1 vs. 1.4% for measurement). Moreover, there is a strong correlation between the simulated and observed iron fractional solubility (R^2=0.67). It is more difficult to predict the absolute amount of soluble iron near the source regions. The model significantly underestimates total soluble iron concentration (0.5–8.3 ng m^{-3} for Exp1) at the GOSAN site (3–98 ng m^{-3} for measurement) which is located between the source areas and remote conditions with a great gradient in concentration (Chen et al., 1997). It is probably because the coarse horizontal resolution of the global model does not account for the distinctive local geography and spatial variability, which could significantly affect the comparisons with the point-based daily measurements.

In our model, faster removal of larger particles leads to larger fractions of fine particles in total aerosols over the remote ocean (i.e., more soluble iron from combustion sources). Additionally, the buffering capacity of mineral aerosol in the fine mode is consumed more efficiently due to the preferential condensation of acids on smaller particles. As a result, the global model simulates higher iron fractional solubility for the fine mode (diameter <2.5 μm) than that for the coarse mode (diameter >2.5 μm) along the atmospheric transport to the eastern North Pacific Ocean. The onboard cruise measurements have reported that smaller particles have higher iron fractional solubility in the tropical Pacific Ocean between 24° N–28° N and 170° E–155° W from 9 to 26 April 2001 (Chen and Siefert, 2003; Hand et al., 2004). In our model simulations, the averaged iron fractional solubility for the fine mode is also higher than that for the coarse mode in the regions of the cruise track (Table 3). When the alkaline dust chemistry is included (Exp1), the model estimate of the iron fractional solubility is in good agreement with measurements (0.5% vs. 0.6±0.2%) for the coarse mode, while the model underestimates for the fine mode (0.8% vs. 1.7±0.8%). If the buffering ability of alkaline dust is neglected (Exp2), better agreement is obtained for the fine mode (2.3%), but the model significantly overestimates for the coarse mode (2.1%). These results may suggest that the iron-containing dust in the coarse mode is likely associated with calcite-rich dust, which is internally mixed with the hematite. On the other hand, the iron-containing dust in the fine mode is possibly associated with aluminosilicate-rich minerals including iron substituted in the crystal lattice of alminosilicates, which are externally mixed with alkaline carbonate minerals. Based on these two model experiments, we propose that smaller dust particles may yield increased amounts of soluble iron relative to larger particles due to possible variations in mixing state of alkaline dust as a non-linear function of iron-containing aerosol particle size. We note that some dust particles in the atmosphere are mineral aggregates composed of two or more minerals, such as aggregates of alminosilicate and gypsum, alminosilicate and calcite, and alminosilicate and iron oxides (Falkovich et al., 2001; Gao and Anderson, 2001; Shi et al., 2005). However, the representation of aggregation process of individual soil

ACPD
10, 10399–10428, 2010

particles with different materials as well as chemical process of iron dissolution for different composition can be very complex and challenging for modeling. Thus, achieving a predictive capability for size-segregated aerosols of soluble iron will require further work involving laboratory experiments, modeling, and observations, such as spatial distribution of iron content in clays, size distribution data of chemical composition in mineral aerosols, and dissolution rates of iron from clay minerals.

3.3 Soluble iron deposition

In addition to mineral dust aerosols, iron from combustion sources could have a pronounced effect on aerosol iron solubility (Chuang et al., 2005; Luo et al., 2008; Schroth et al., 2009). Nevertheless, we estimate (Exp1) that monthly averaged soluble iron deposition from dust source is significantly higher (5–7.5 $\mathrm{pg\,m^{-2}\,s^{-1}}$ for Exp1 in Fig. 6a) than that from the combustion source (0.5–1.0 $\mathrm{pg\,m^{-2}\,s^{-1}}$ in Fig. 6b) over the eastern North Pacific Ocean.

This simulation (Exp1), however, underestimated the mass fraction of soluble iron in the fine mode to the total soluble iron concentration (54% for Exp1 vs. 79% for measurement in Table 3) over the Pacific Ocean. If we combine the iron deposition for fine particles from Exp2 (aluminosilicate-rich dust) with that for coarse particles from Exp1 (calcite-rich dust), we would be able to obtain a better agreement in the mass fraction (75%) with the observation. The combined data set (Fig. 6c) is based on the assumption that dust mineralogy could be different in the fine and coarse modes. It may be interesting for a sensitivity simulation in ocean biogeochemistry model, because no previous atmospheric model could reproduce the inverse relationship between aerosol iron solubility and particle size quantitatively. The mass fraction of dust in the fine-mode aerosols is small near the source regions, so that the resulted increases in iron deposition are small near the continents. However, it is noteworthy that the deposition of soluble iron from this scenario would become predominantly high (10–15 $\mathrm{pg\,m^{-2}\,s^{-1}}$) over the eastern North Pacific Ocean, due to a longer residence time of smaller particles.

4 Summary and conclusions

We investigated the impact of alkaline dust on the acid mobilization of iron. In order to do that, we introduced a specific mineral dissolution component to the global aerosol chemistry transport model. We have compiled the soluble iron emission data set from both dust and combustion sources. Through this study, we demonstrated that most alkaline dusts cannot be entirely consumed by acids during transport across the North Pacific Ocean. The mixing state of iron-containing aerosols with alkaline carbonate minerals and subsequent atmospheric chemical processing of the aerosols resulted in substantial differences in the iron solubility. The inclusion of alkaline dust in aqueous chemistry significantly limits the iron dissolution by inorganic acids in aerosol solution during the long-range transport. However, deserts in East Asia are still the dominant sources to the ocean deposition of total soluble iron over the N. Pacific.

Our results suggest that the iron dissolved from hematite in calcite-rich dust could be lower than that previously estimated, while aluminosilicate-rich minerals might provide a highly-soluble aerosol iron due to the strong acid mobilization of iron. Taking into account of this non-linearity, we have improved our ability to estimate the iron fractional solubility in different particle sizes; but quantitative, episodic, and predictive capabilities of the soluble iron remain a challenge. Using this scenario, we showed that the deposition of soluble iron from smaller dust particles could be a dominant source of bioavailable iron over the eastern North Pacific Ocean. Thus while much of the research on understanding the role of mineral-dust iron in ocean productivity has focused on larger dust particles, further work would be required to study the atmospheric processing of mineral aerosols for different size modes in conjunction with size-fractionated mineralogy.

Conventionally, dust is assumed as the major supply of bioavailable iron with a constant solubility at 1–2% to the remote ocean, while Krishnamurthy et al. (2009) employed dust and combustion sources of Luo et al. (2008) with a 50% reduction (from 4% to 2%) in combustion iron initial solubility. However, the timing and location of the

ACPD
10, 10399–10428, 2010

atmospheric input to the ocean may be different from those previously assumed. Past and future changes in aerosol supply of bioavailable iron might affect the availability of nutrients for phytoplankton production in the upper ocean, as global warming has been predicted to intensify stratification and reduce vertical mixing. Thus the feedback of climate change through ocean uptake of CO_2 as well as via aerosol-cloud interaction, which may be induced by sulfate formation from dimethylsulfide (DMS) and carbon-containing aerosols production from the ocean biomass, might be modified by the inclusion of bioavailable iron deposition.

Acknowledgements. Support for this research was provided to A. Ito by Innovative Program of Climate Change Projection for the 21st Century (MEXT) and to Y. Feng by National Science Foundation (NSF), Atmospheric Sciences Program, under the grant ATM-0721142.

References

Andronova, A. V., Gomes, L., Smirnov, V. V., Ivanov, A. V., and Shukurova, L. M.: Physico-chemical characteristics of dust aerosols deposited during the Soviet-American eperiment (Tajikistan, 1989), Atmos. Environ., Part A: General Topics, 27(16), 2487–2493, 1993.

Arimoto, R., Zhang, X. Y., Huebert, B. J., Kang, C. H., Savoie, D. L., Prospero, J. M., Sage, S. K., Schloesslin, C. A., Khaing, H. M., and Oh, S. N.: Chemical composition of atmospheric aerosols from Zhenbeitai, China, and Gosan, South Korea, during ACE-Asia, J. Geophys. Res., 109(D19), D19S04, doi:10.1029/2003JD004323, 2004.

Azuma, K. and Kametani, H.: Kinetics of dissolution of ferric oxide, Trans. Metall. Soc. AIME, 230, 853–862, 1964.

Baker, A. R. and Croot, P. L.: Atmospheric and marine controls on aerosol iron solubility in seawater, Mar. Chem., in press, doi:10.1016/j.marchem. 2008.09.003, 2008.

Baker, A. R. and Jickells, T. D.: Mineral particle size as a control on aerosol iron solubility, Geophys. Res. Lett., 33, L17608, doi:10.1029/2006GL026557, 2006.

Blesa, M. A., Morando, P. J., and Regazzoni, A. E.: Chemical Dissolution of Metal Oxides, 401 pp., CRC Press, Boca Raton, Fla, 1994.

Buck, C. S., Landing, W. M., and Resing, J. A.: Particle size and aerosol iron

solubility: A high-resolution analysis of Atlantic aerosols, Mar. Chem., in press, doi:10.1016/j.marchem.2008.11.002, 2008.
Burch, T. E., Nagy, K. L., and Lasaga, A. C.: Free energy dependence of albite dissolution kinetics at 80_C and pH 8.8, Chem. Geol., 105(1–3), 137–162, 1993.
Cama, J., Ayora, C., and Lasaga, A. C.: The deviation-from-equilibrium effect on dissolution rate and on apparent variations in activation energy, Geochim. Cosmochim. Acta, 63(17), 2481–2486, 1999.
Chen, L.-L., Carmichael, G. R., and Hong, M.-S., et al.: Influence of continental outflow events on the aerosol composition at Cheju Island, South Korea, J. Geophys. Res., 102, 28551–28574, 1997.
Chen, Y. and Siefert, R.: Determination of various types of labile atmospheric iron over remote oceans, J. Geophys. Res., 108(D24), 4774, doi:10.1029/2003JD003515, 2003.
Chou, L., Garrels, R. M., and Wollast, R.: Comparative study of the kinetics and mechanisms of dissolution of carbonate minerals, Chem. Geol., 78, 269–282, 1989.
Chuang, P. Y., Duvall, R. M., Shafer, M. M., and Schauer, J. J.: The origin of water soluble particulate iron in the Asian atmospheric outflow, Geophys. Res. Lett., 32, L07813, doi:10.1029/2004GL021946, 2005.
Claquin, T., Schulz, M., and Balkanski, Y. J.: Modeling the mineralogy of atmospheric dust sources, J. Geophys. Res., 104, 22243–22256, 1999.
Cornell, R. M. and Schwertmann, U.: The Iron Oxides: Structure, Properties, Reactions, Occurrences and Uses, 573 pp., John Wiley, Hoboken, N. J., 1996.
Cwiertny, D. M., Baltrusaitis, J., Hunter, G. J., Laskin, A., Scherer, M. M., and Grassian, V. H.: Characterization and acid-mobilization study of iron-containing mineral dust source materials, J. Geophys. Res., 113, D05202, doi:10.1029/2007JD009332, 2008.
Dentener, F. J., Carmichael, G. R., Zhang, Y., Lelieveld, J., and Crutzen, P. J.: Role of mineral aerosol as a reactive surface in the global troposphere, J. Geophys. Res., 101(D17), 22869–22889, 1996.
Dentener, F., Kinne, S., Bond, T., Boucher, O., Cofala, J., Generoso, S., Ginoux, P., Gong, S., Hoelzemann, J. J., Ito, A., Marelli, L., Penner, J. E., Putaud, J.-P., Textor, C., Schulz, M., van der Werf, G. R., and Wilson, J.: Emissions of primary aerosol and precursor gases in the years 2000 and 1750 prescribed data-sets for AeroCom, Atmos. Chem. Phys., 6, 4321–4344, 2006, http://www.atmos-chem-phys.net/6/4321/2006/.

Duce, R. A. and Tindale, N. W.: Atmospheric transport of iron and its deposition in the ocean, Limnol. Oceanogr., 36(8), 1715–1726, 1991.
Duvall, R. M., Majestic, B. J., Shafer, M. M., Chuang, P. Y., Simoneit, B. R. T., and Schauer, J. J.: The water-soluble fraction of carbon, sulfur, and crustal elements in Asian aerosols and Asian soils, Atmos. Environ., 42, 5872–5884, 2008.
Fairlie, T. D., Jacob, D. J., Dibb, J. E., Alexander, B., Avery, M. A., van Donkelaar, A., and Zhang, L.: Impact of mineral dust on nitrate, sulfate, and ozone in transpacific Asian pollution plumes, Atmos. Chem. Phys. Discuss., 9, 24477–24510, 2009, http://www.atmos-chem-phys-discuss.net/9/24477/2009/.
Falkovich, A. H., Ganor, E., Levin, Z., Formenti, P., and Rudich, Y.: Chemical and mineralogical analysis of individual mineral dust particles, J. Geophys. Res., 106, 18029–18036, 2001.
Feng, Y. and Penner, J. E.: Global modeling of nitrate and ammonium: Interaction of aerosols and tropospheric chemistry, J. Geophys. Res., 112, D01304, doi:10.1029/2005JD006404, 2007.
Fung, I. Y., Meyn, S. K., Tegen, I., Doney, S. C., John, J. G., and Bishop, J. K. B.: Iron supply and demand in the upper ocean, Global Biogeochem. Cycles, 14(2), 697–700, 2000.
Gao, Y. and Anderson, J. R.: Characteristics of Chinese aerosols determined by individual-particle analysis, J. Geophys. Res., 106, 18037–18045, 2001.
Gillette, D. A., Patterson Jr., E. M., Prospero, J. M., and Jackson, M. L.: Soil aerosols, in Aerosol Effects on Climate, edited by S. G. Jennings, pp. 77–109, Univ. of Ariz., Tucson, 1993.
Guieu, C., Bonnet, S., Wagener, T., and Loye-Pilot, M.-D.: Biomass burning as a source of dissolved iron to the open ocean?, Geophys. Res. Lett., 22, L19608, doi:10.1029/2005GL022962, 2005.
Hand, J. L., Mahowald, N. M., Chen, Y., Siefert, R. L., Luo, C., Subramaniam, A., and Fung, I.: Estimates of atmospheric-processed soluble iron from observations and a global mineral aerosol model: Biogeochemical implications, J. Geophys. Res., 109, D17205, doi:10.1029/2004JD004574, 2004.
Hildemann, L., Markowski, G., and Cass, G.: Chemical composition of emissions from urban sources of fine organic aerosol, Environ. Sci. Technol., 25, 744–759, 1991.
Ito, A. and Penner, J. E.: Historical emissions of carbonaceous aerosols from biomass and fossil fuel burning for the period 1870–2000, Global Biogeochem. Cycles, 19, GB2028, doi:10.1029/2004GB002374, 2005.
Ito, A., Sillman, S., and Penner, J. E.: Effects of additional nonmethane volatile organic com-

pounds, organic nitrates, and direct emissions of oxygenated organic species on global tropospheric chemistry, J. Geophys. Res., 112, D06309, doi:10.1029/2005JD006556, 2007.
Ito, A., Sillman, S., and Penner, J. E.: Global chemical transport model study of ozone response to changes in chemical kinetics and biogenic volatile organic compounds emissions due to increasing temperatures: Sensitivities to isoprene nitrate chemistry and grid resolution, J. Geophys. Res., 114, D09301, doi:10.1029/2008JD011254, 2009.
Iwasaka, Y., Yamato, M., Imasu, R., and Ono, A.: Transport of Asian dust (KOSA) particles: importance of weak KOSA events on the geochemical cycle of soil particles, Tellus, 40B, 494–503, 1988.
Jacobson, M. Z.: Studying the effects of calcium and magnesium on size-distributed nitrate and ammonium with EQUISOLV II, Atmos. Environ., 33, 3635–3649, 1999.
Jickells, T. D., An, Z. S., Andersen, K. K., et al.: Global iron connections between desert dust, ocean biogeochemistry, and climate, Science, 308, 67–71, 2005.
Journet, E., Desboeufs, K. V., Caquineau, S., and Colin, J.-L.: Mineralogy as a critical factor of dust iron solubility, Geophys. Res. Lett., 35, L07805, doi:10.1029/2007GL031589, 2008.
Krishnamurthy, A., Moore, J. K., Mahowald, N., Luo, C., Doney, S. C., Lindsay, K., and Zender, C. S.: Impacts of increasing anthropogenic soluble iron and nitrogen deposition on ocean biogeochemistry, Global Biogeochem. Cycles, 23, GB3016, doi:10.1029/2008GB003440, 2009.
Lasaga, A. C., Soler, J. M., Ganor, J., Burch, T. E., and Nagy, K. L.: Chemical-weathering rate laws and global geochemical cycles, Geochim. Cosmochim. Acta, 58(10), 2361–2386, 1994.
Liu, X., Penner, J. E., and Herzog, M.: Global modeling of aerosol dynamics: Model description, evaluation and interactions between sulfate and non-sulfate aerosols, J. Geophys. Res., 110, D18206, doi:10.1029/2004JD005674, 2005.
Luo, C., Mahowald, N., Bond, T., Chuang, P. Y., Artaxo, P., Siefert, R., Chen, Y., and Schauer, J.: Combustion iron distribution and deposition, Global Biogeochem. Cycles, 22, GB1012, doi:10.1029/2007GB002964, 2008.
Maenhaut, W., Salma, I., Cafmeyer, J., Annegarn, H. J., and Andreae, M. O.: Regional atmospheric aerosol composition and sources in the eastern Transvaal, South Africa, and impact of biomass burning, J. Geophys. Res., 101, 23631–23650, 1996.
Mahowald, N. M., Sebastian, E., Luo, C., et al.: Atmospheric iron deposition: global distribution, variability, and human perturbations, Annu. Rev. Mar. Sci., 1, 245–278, 2009.

Mamane, Y., Miller, J., and Dzubay, T.: Characterization of individual fly ash particles emitted from coal- and oil-fired power plants, Atmos. Environ., 20, 2125–2135, 1986.
Mamuro, T., Mizohata, A., and Kubota, T.: Elemental composition of suspended particles released from various boilers, J. Jpn. Soc. Air Pollut., 14, 296–303, 1979a (in Japanese).
Mamuro, T., Mizohata, A., and Kubota, T.: Elemental composition of suspended particles released in refuse incineration, J. Jpn. Soc. Air Pollut., 14, 190–196, 1979b (in Japanese).
Mamuro, T., Mizohata, A., and Kubota, T.: Elemental composition of suspended particles released from iron and steel works, J. Jpn. Soc. Air Pollut., 15, 69–76, 1980 (in Japanese).
Martin, J. H., Coale, K. H., Johnson, K. S., et al.: Testing the iron hypothesis in ecosystems of the equatorial Pacific Ocean, Nature, 371, 123–129, 1994.
Maxwell-Meier, K., Weber, R., Song, C., Orsini, D., Ma, Y., Carmichael, G. R., and Streets, D. G.: Inorganic composition of fine particles in mixed mineral dust–pollution plumes observed from airborne measurements during ACE-Asia, J. Geophys. Res., 109, D19S07, doi:10.1029/2003JD004464, 2004.
McNaughton, C. S., Clarke, A. D., Kapustin, V., Shinozuka, Y., Howell, S. G., Anderson, B. E., Winstead, E., Dibb, J., Scheuer, E., Cohen, R. C., Wooldridge, P., Perring, A., Huey, L. G., Kim, S., Jimenez, J. L., Dunlea, E. J., DeCarlo, P. F., Wennberg, P. O., Crounse, J. D., Weinheimer, A. J., and Flocke, F.: Observations of heterogeneous reactions between Asian pollution and mineral dust over the Eastern North Pacific during INTEX-B, Atmos. Chem. Phys., 9, 8283–8308, 2009, http://www.atmos-chem-phys.net/9/8283/2009/.
Meng, Z., Seinfeld, J. H., Saxena, P., and Kim, Y. P.: Atmospheric gas aerosol equilibrium: IV. Thermodynamics of carbonates, Aerosol Sci. Technol., 23, 131–154, 1995.
Meskhidze, N., Chameides, W. L., Nenes, A., and Chen, G.: Iron mobilization in mineral dust: Can anthropogenic SO_2 emissions affect ocean productivity?, Geophys. Res. Lett., 30(21), 2085, doi:10.1029/2003GL018035, 2003.
Meskhidze, N., Chameides, W. L., and Nenes, A.: Dust and pollution: A recipe for enhanced ocean fertilization?, J. Geophys. Res., 110, D03301, doi:10.1029/2004JD005082, 2005.
Mills, M. M., Ridame, C., Davey, M., La Roche, J., and Geider, R. J.: Iron and phosphorus co-limit nitrogen fixation in the eastern tropical north Atlantic, Nature, 429, 292–294, 2004.
Nishikawa, M., Kanamori, S., Kanamori, N., and Mizoguchi, T.: Kosa aerosol as eolian carrier of anthropogenic material, Sci. Total Environ., 107, 13–27, 1991.
Olmez, I., Sheffield, A., Gordon, G., Houck, J., Pritchett, L., Cooper, J., Dzubay, T. G., and

Bennett, R.: Compositions of particles from selected sources in Philadelphia for receptor modeling applications, J. Air Pollut. Control Assoc., 38, 1392–1402, 1988.
Pokrovsky, O. S. and Schott, J.: Processes at the magnesium-bearing carbonates/solution interface. II. Kinetics and mechanism of magnesite, Geochim. Cosmochim. Acta, 63, 881–897, 1999.
Rotman, D. A., Atherton, C. S., Bergmann, D. J., et al.: IMPACT, the LLNL 3-D global atmospheric chemical transport model for the combined troposphere and stratosphere: Model description and analysis of ozone and other trace gases, J. Geophys. Res., 109, D04303, doi:10.1029/2002JD003155, 2004.
Schroth, A. W., Crusius, J., Sholkovitz, E. R., and Bostick, B. C.: Iron solubility driven by speciation in dust sources to the ocean, Nat. Geosci., 2, 337–340, doi:10.1038/ngeo501, 2009.
Sedwick, P. N., Sholkovitz, E. R., and Church, T. M.: Impact of anthropogenic combustion emissions on the fractional solubility of aerosol iron: Evidence from the Sargasso Sea, Geochem. Geophys. Geosyst., 8, Q10Q06, doi:10.1029/2007GC001586, 2007.
Shao, L. Y., Li, W. J., Yang, S. S., Shi, Z. B., and Lü, S. L.: Mineralogical characteristics of airborne particles collected in Beijing during a severe Asian dust storm period in spring 2002, Science in China(D), 50(6), 953–959, 2007.
Shi, Z., Shao, L., Jones, T. P., and Lu, S.: Microscopy and mineralogy of airborne particles collected during severe dust storm episodes in Beijing, China, J. Geophys. Res., 110, D01303, doi:10.1029/2004JD005073, 2005.
Shi, Z., Krom, M. D., Bonneville, S., Baker, A. R., Jickells, T. D., and Benning, L. G.: Formation of iron nanoparticles and increase in iron reactivity in mineral dust during simulated cloud processing, Environ. Sci. Technol., 43, 6592–6596, 2009.
Sholkovitz, E. R., Sedwick, P. N., and Church, T. M.: Influence of anthropogenic combustion emissions on the deposition of soluble aerosol iron to the ocean: Empirical estimates for island sites in the North Atlantic, Geochim. Cosmochim. Acta, 73, 3981–4003, 2009.
Siefert, R. L., Johansen, A. M., and Hoffmann, M. R.: Chemical characterization of ambient aerosol collected during the southwest monsoon and intermonsoon seasons over the Arabian Sea: Labile-Fe(II) and other trace metals, J. Geophys. Res., 104, 3511–3526, 1999.
Skopp, J. M.: Physical properties of primary particles, in: Handbook of Soil Science, edited by: Summer, M. E., pp. 3–17, CRC Press, Boca Raton, Fla., 2000.
Smith, R., Campbell, J., and Nielson, K.: Characterization and formation of submicron particles

in coal-fired plants, Atmos. Environ., 13, 607–617, 1979.
Solmon, F, Chuang, P. Y., Meskhidze, N., and Chen, Y.: Acidic processing of mineral dust iron by anthropogenic compounds over the North Pacific Ocean, J. Geophys. Res., 114, D02305, doi:10.1029/2008JD010417, 2009.
Song, C. H. and Carmichael, G. R.: The aging process of naturally emitted aerosol (sea-salt and mineral aerosol) during long range transport, Atmos. Environ., 33(14), 2203–2218, 1999.
Song, C. H. and Carmichael, G. R.: Gas-particle partitioning of nitric acid modulated by alkaline aerosol, J. Atmos. Chem., 40(1), 1–22, 2001.
Streets, D. G., Bond, T. C., Carmichael G. R., et al.: An inventory of gaseous and primary aerosol emissions in Asia in the year 2000, J. Geophys. Res., 108(D21), 8809, doi:10.1029/2002JD003093, 2003.
Sullivan, R. C., Guazzotti, S. A., Sodeman, D. A., and Prather, K. A.: Direct observations of the atmospheric processing of Asian mineral dust, Atmos. Chem. Phys., 7, 1213–1236, 2007, http://www.atmos-chem-phys.net/7/1213/2007/.
Sun, J., Chang, M., and Liu, T.: Spatial and temporal characteristics of dust storms in China and its surrounding regions, 1960–1999: Relations to source area and climate, J. Geophys. Res., 106, 18331–18344, 2001.
Tang, Y. H., Carmichael, G. R., Seinfeld, J. H., et al.: Three-dimensional simulations of inorganic aerosol distributions in east Asia during spring 2001, J. Geophys. Res., 109, D19S23, doi:10.1029/2003JD004201, 2004.
Turn, S. Q., Jenkins, B. M., Chow, J. C., Pritchett, L. C., Cambell, D., Cahill, T., and Whalen, S. A.: Elemental characterization of particulate matter emitted from biomass burning: Wind tunnel derived source profiles for herbaceous and wood fuels, J. Geophys. Res., 102, 3683–3699, 1997.
Ward, D. E., Setzer, A. W., Kaufman, Y. J., and Rasmussen, R. A.: Characteristics of smoke emissions from biomass fires of the Amazon region – BASE-A experiment, in: Global Biomass Burning: Atmospheric, Climatic, and Biospheric Implications, edited by: Levine, J. S., pp. 394–402, MIT Press, Cambridge, MA, 1991.
Ward, D. E., Susott, R. A., Kauffman, J. B., Babbitt, R. E., Cummings, D. L., Dias, B., Holben, B. N., Kaufman, Y. J., Rasmussen, R. A., and Setzer, A. W.: Smoke and fire characteristics for cerrado and deforestation burns in Brazil: BASE-B experiment, J. Geophys. Res., 97, 14601–14619, 1992.

Yamasoe, M. A., Artaxo, P., Miguel, A. H., and Allen, A. G.: Chemical composition of aerosol particles from direct emissions of vegetation fires in the Amazon Basin: Water-soluble species and trace elements, Atmos. Environ., 34, 1641–1653, 2000.

Zhang, D., Shi, G.-Y., Iwasaka, Y., and Hu, M.: Mixture of sulfate and nitrate in coastal atmospheric aerosols: Individual particle studies in Qingdao (36°04′ N, 120°21′ E), China, Atmos. Environ., 34, 2669–2679, 2000.

Zhu, X. R., Prospero, J. M., Millero, F. J., Savoie, D. L., and Brass, G. W.: The solubility of ferric ion in marine mineral aerosol solutions at ambient relative humidities, Mar. Chem., 38, 91–107, 1992.

Zhuang, G., Yi, Z., Duce, R. A., and Brown, P. R.: Link between iron and sulphur cycles suggested by detection of Fe(II) in remote marine aerosols, Nature, 355, 537–539, 1992.

Zinder, B., Furrer, G., and Stumm, W.: The coordination chemistry of weathering: II. Dissolution of Fe(III) oxides, Geochim. Cosmochim. Acta, 50(9), 1861–1869, 1986.

Table 1. Constants used to calculate mineral dissolution/precipitation rates.

Number	Mineral	Rate Constant K_i ($mol_{mineral\ dissolved}\ m^{-2}\ s^{-1}$)	m_i	A_i ($m^2\ g^{-1}$)	W_i (%)	Reference
RS1	Calcite	Equilibrium				Meng et al. (1995)
RS2	Magnesite	4.4×10^{-5}exp[2400(1/298–1/T)]	1.0	1.0	5.5	Chou et al. (1989)
RS3	Hematite	Stage I (0–0.8% of total oxide dissolved)	0.5	100	5.0	Azuma and Kametani (1964);
		4.4×10^{-12}exp[9200(1/298–1/T)]				Blesa et al. (1994);
		Stage II (0.8–40% of total oxide dissolved)				Cornell and Schwertmann (1996)
		1.8×10^{-11}exp[9200(1/298–1/T)]				Skopp (2000); Zinder et al. (1986)
		Stage III (40–100% of total oxide dissolved)				
		3.5×10^{-12}exp[9200(1/298–1/T)]				

ACPD
10, 10399–10428, 2010

Table 2. Iron fractions in minerals.

Source	Fine (%)	Coarse (%)	Reference
	Fossil fuels		
Coal: power/industrial	7.5	9.4	Mamane et al. (1986)
	7.6	8.1	Olmez et al. (1988)
	4.5		Smith et al. (1979)
Value used	6.5	8.7	
Coal: residential	0.1	0.1	Luo et al. (2008)
Coal briquettes	1.6		Luo et al. (2008)
Oil boiler	0.13		Hildemann et al. (1991)
	1.7		Mamane et al. (1986)
	0.41	0.46	Mamuro et al. (1979a)
	1.6	2.95	Olmez et al. (1988)
Value used	0.96	1.16	
iron and steel	1.22	15.7	Mamuro et al. (1980)
	Biofuels		
Agricultural wastes	0.017	0.13	Turn et al. (1997)
Fuelwood	0.0058	0.026	Turn et al. (1997)
	Waste		
incinerator	0.59	0.61	Mamuro et al. (1979b)
	0.22	1.7	Olmez et al. (1988)
Value used	0.36	1.02	
	Biomass burning		
Savanna	0.020		Maenhaut et al. (1996)
Savanna	0.030		Maenhaut et al. (1996)
Ceraddo	0.900		Ward et al. (1991)
Ceraddo	1.200		Ward et al. (1992)
Ceraddo	0.077		Yamasoe et al. (2000)
Ceraddo	0.045		Yamasoe et al. (2000)
Extratropical forest	0.100		Ward et al. (1991)
Tropical forest	0.900		Ward et al. (1991)
Tropical forest	0.100		Ward et al. (1992)
Tropical forest	0.031		Yamasoe et al. (2000)
Tropical forest	0.048		Yamasoe et al. (2000)
Tropical forest	0.100		Yamasoe et al. (2000)
		3.4	Luo et al. (2008)
Value used	0.296	3.4	

ACPD

10, 10399–10428, 2010

Table 3. Observed and modeled iron fractional solubility and soluble iron concentration for the fine mode and coarse mode (mean±standard deviation).

Location	GOSAN (33°17′ N, 126°10′ E)		Cruise (24°N–28° N, 170° E–155° W)	
Particle size	Bulk	Bulk	Fine	Coarse
Number of data	27	23[a]	18	18
	Iron fractional solubility (%)			
Observations	2.6±3.3	1.4±1.2	1.7±0.8	0.6±0.2
Exp1[b]	1.4±0.6	1.4±0.6	0.82±0.15	0.54±0.02
Exp2[c]	2.0±0.7	1.9±0.7	2.3±0.16	2.1±0.2
	Soluble iron concentration (ng m^{-3})			
Observations	32±23	26±15	1.1±1.2	0.3±0.2
Exp1[b]	3.8±2.1	3.9±2.2	0.13±0.17	0.11±0.13
Exp2[c]	5.7±3.3	5.7±3.5	0.33±0.37	0.42±0.47

[a] Four distinct high values of the water-soluble fraction of iron in the total suspended particles were excluded.
[b] Alkaline dust aerosols are internally mixed with the iron-containing minerals.
[c] Alkaline dust aerosols are externally mixed with the iron-containing minerals.

ACPD
10, 10399–10428, 2010

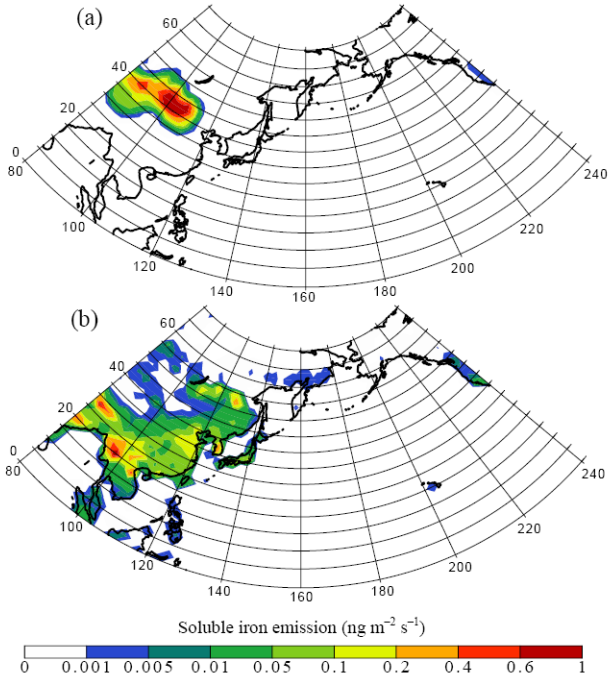

Fig. 1. Spatial distribution of monthly averaged soluble iron emission (ng m^{-2} s^{-1}) from **(a)** desert and **(b)** combustion sources in April.

ACPD
10, 10399–10428, 2010

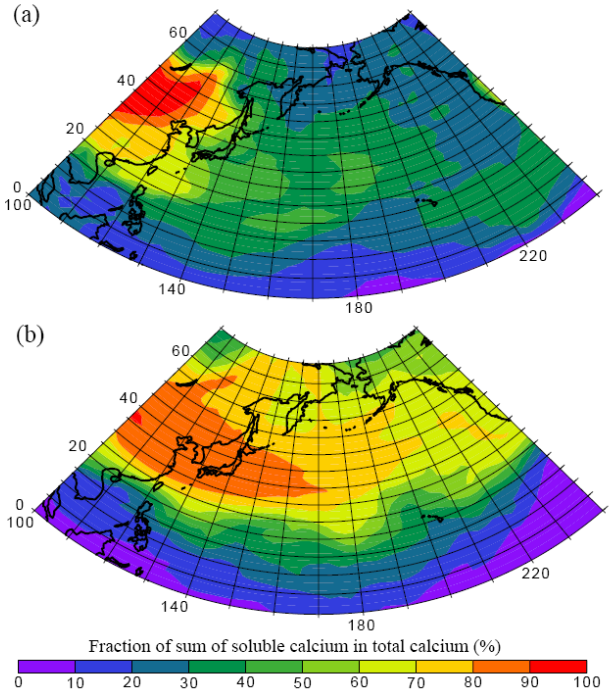

Fig. 2. Spatial distribution of soluble calcium in total calcium (%) in **(a)** the surface air and **(b)** the free troposphere during April 2001.

ACPD

10, 10399–10428, 2010

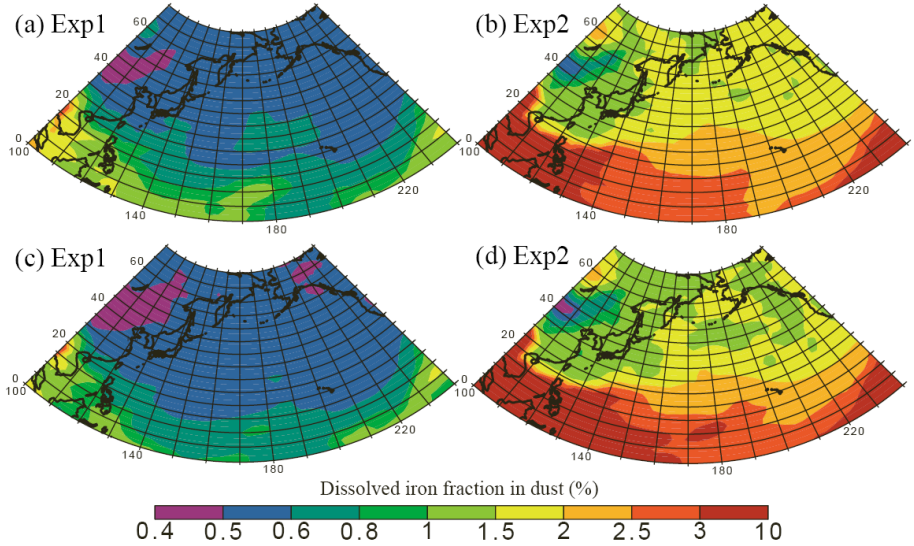

Fig. 3. Modeled dissolved iron fraction (DIF) in dust (%) in the surface air during April 2001 for **(a)** the fine mode with the alkaline dust, **(b)** the fine mode without the alkaline dust, **(c)** the coarse mode with the alkaline dust, and **(d)** the coarse mode without the alkaline dust.

ACPD
10, 10399–10428, 2010

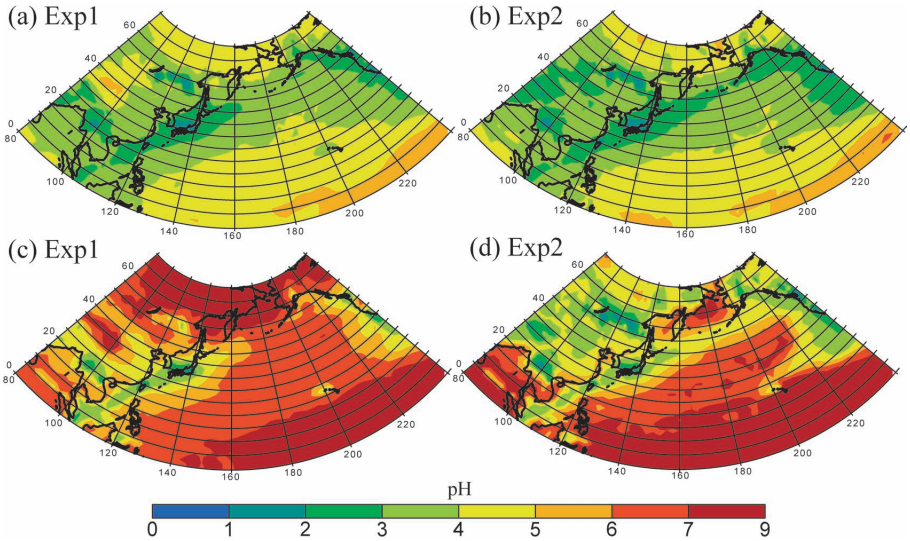

Fig. 4. Modeled pH in aerosols in the surface air during April 2001 for **(a)** the fine mode with the alkaline dust, **(b)** the fine mode without the alkaline dust, **(c)** the coarse mode with the alkaline dust, and **(d)** the coarse mode without the alkaline dust.

ACPD
10, 10399–10428, 2010

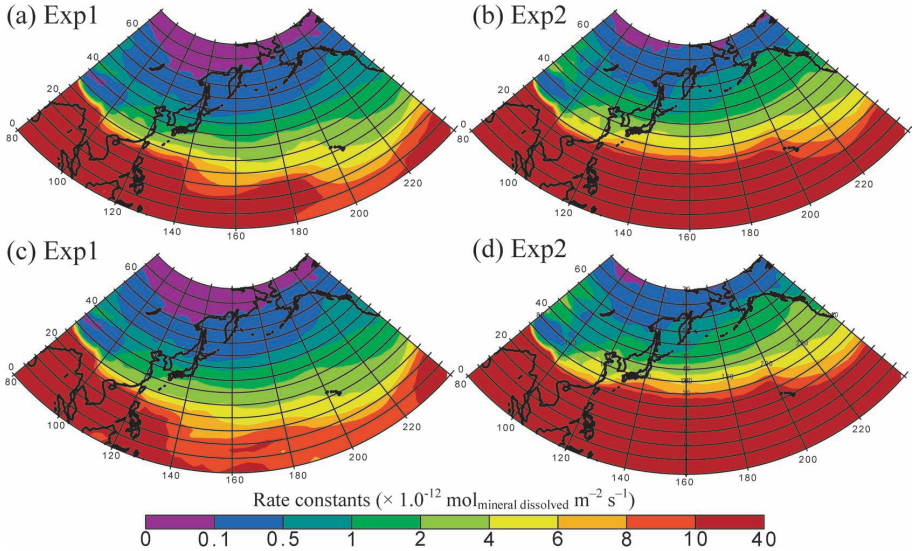

Fig. 5. Modeled dissolution rate constants ($\times 1.0^{-12}$ $mol_{mineral\ dissolved}$ m^{-2} s^{-1}) for hematite (RS3) in the surface air during April 2001 for **(a)** the fine mode with the alkaline dust, **(b)** the fine mode without the alkaline dust, **(c)** the coarse mode with the alkaline dust, and **(d)** the coarse mode without the alkaline dust.

ACPD
10, 10399–10428, 2010

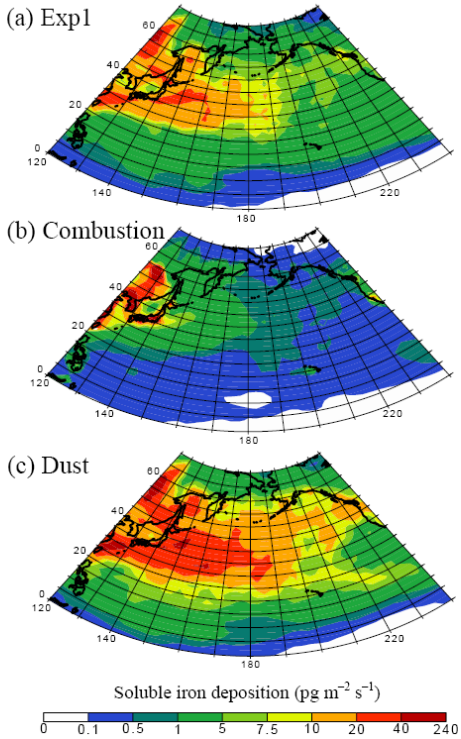

Fig. 6. Monthly averaged soluble iron deposition (pg m^{-2} s^{-1}) to the ocean from **(a)** dust source (Exp1), **(b)** combustion source, and **(c)** dust source with combination of Exp1 for coarse mode and Exp2 for fine mode during April 2001.

ACPD
10, 10399–10428, 2010